

# Searching towards Class-Aware Generators for Conditional Generative Adversarial Networks

Peng Zhou<sup>1</sup>, Lingxi Xie<sup>2</sup>, Xiaopeng Zhang<sup>2</sup>, Bingbing Ni<sup>1</sup>, Qi Tian<sup>2</sup>

<sup>1</sup>Shanghai Jiao Tong University, <sup>2</sup>Huawei Inc.

zhoupengcv@sjtu.edu.cn, 198808xc@gmail.com, zxphistory@gmail.com,  
nibingbing@sjtu.edu.cn, tian.qi1@huawei.com

## Abstract

Conditional Generative Adversarial Networks (cGAN) were designed to generate images based on the provided conditions, *e.g.*, class-level distributions. However, existing methods have used the same generating architecture for all classes. This paper presents a novel idea that adopts NAS to find a distinct architecture for each class. The search space contains regular and class-modulated convolutions, where the latter is designed to introduce class-specific information while avoiding the reduction of training data for each class generator. The search algorithm follows a weight-sharing pipeline with mixed-architecture optimization so that the search cost does not grow with the number of classes. To learn the sampling policy, a Markov decision process is embedded into the search algorithm and a moving average is applied for better stability. We evaluate our approach on CIFAR10 and CIFAR100. Besides demonstrating superior performance, we deliver several insights that are helpful in designing efficient GAN models. Code is available<sup>1</sup>.

## 1 Introduction

The Generative Adversarial Network (GAN) algorithm [14] has attracted considerable attention and achieved great success in image generation. The key challenge of GAN is to adjust the high-dimensional data distributions under different scenarios, *e.g.*, by noticing that the semantic class can largely impact data distribution, researchers designed the conditional version of GAN (*i.e.*, cGAN [28]), that introduced class information to the network via a class-conditional vector and achieved better performance [29]. The success of cGAN motivates us to think over a more flexible design that the architecture of generators can be different across classes. We notice that state-of-the-art GAN algorithms have not used this configuration, despite that multiple generators have been used in some algorithms [17, 2, 12].

In this paper, we investigate the possibility of designing class-aware generators. To explore the exponentially many combinations, we adopt neural architecture search (NAS) methods. However, this is a challenging task in several aspects. In particular, as the number of classes increases, training an individual generator for each class is rather cumbersome and incurs the lack of sufficient training data for each class generator. Our solution involves two key contributions.

**First**, we present a carefully designed search space that is both flexible and safe. We refer to flexibility as the ability to assign a distinct generator architecture to each class, which makes the search space exponentially large. To guarantee that generators of different classes can share the limited amount of training data, we reduce the variation between different architectures by introducing a new operator named class-modulated convolution (*CMconv*), which shares the same set of convolutional weights with the regular convolution but is equipped with a standalone set of weights to modulate the class-conditional input. This space allows the training data to be shared among different architectures and

<sup>1</sup>[https://github.com/PeterouZh/NAS\\_cGAN](https://github.com/PeterouZh/NAS_cGAN)

thus alleviates the empirical risk of optimization, *i.e.*, some operations only belonging to one class cannot be fully trained when there are less training data for the class.

**Second**, we design an efficient search method to explore the search space. This is achieved by a weight-sharing NAS approach with an efficient implementation for mixed-architecture optimization such that the labor cost of training does not increase with the number of classes. A sampling policy is optimized using reinforcement learning, in particular, a Markov decision process (MDP). To suppress the inaccuracy of weight-sharing NAS [6], the MDP is embedded into the search procedure that is equivalent to applying a moving average to the learned policy. Another key factor to the search process is to use a class-conditional discriminator that aligns with the class-aware generators, the discriminator which is critical to deriving distinct class-aware generators.

We perform experiments on some popular benchmarks, including the CIFAR10 and CIFAR100 datasets that have different numbers of classes. For unconditional image generation, our search method shows superior performance, comparable to those equipped with the automatic search [13, 11, 38]. For class-conditional image generation, our approach shows significant gains in terms of important criteria (*e.g.*, FID and intra FIDs). More interestingly, we find that in the best model found by us, the class-modulated convolution is more likely to appear in the early stage (close to the input noise distribution) of the generator. We apply this finding as an empirical rule to BigGAN [3], with a manually designed architecture, and also observe performance gain. This implies that our algorithm delivers useful and generalized insights to the design of GAN models. We will release all code and pre-trained models to facilitate future research.

## 2 Related Work

Generative Adversarial Network (GAN) [14] have demonstrated impressive generation capabilities [20, 3, 21]. Nevertheless, it has notorious issues like vanishing gradient, training instability, and mode collapse. There are a number of improvements for the original GAN, *e.g.*, changing the objective function [1, 15, 27, 18, 33], improving network architecture [34, 3, 21, 9, 42, 19], using multiple generators or discriminators [37, 17, 2, 10, 12, 30]. Recently, the surge in neural architecture search (NAS) has triggered a wave of interest in automatically designing the network architecture of GAN [38, 13, 11].

Conditional GAN (cGAN) [28] is another type of GAN that incorporates class information into the original GAN, so that achieving promising results for the class-sensitive image generation task. Most of the early methods just incorporated the class information by concatenation [28, 35]. AC-GAN [31] incorporated the label information into the objective function of the discriminator by an auxiliary classifier. Miyato and Koyama [29] proposed the class-projection (*cproj*) discriminator, which injected class information into the discriminator in a projection-based way. Furthermore, conditional batch normalization (CBN) [8] is a very effective method to modulate convolutional feature maps by conditional information. Subsequently, *cproj* and CBN are widely used together, forming some powerful cGANs for class image generation [42, 3].

## 3 Our Approach

### 3.1 Motivation of Class-Aware Generators and the Overall Framework

The motivation of our work comes from the existing series of conditional GAN (cGAN) [3, 31, 29] that demonstrates the superiority of introducing class-conditional information to generate images of higher quality. Going one step further, we expect the network to gain the ability of adjusting the generator architecture according to the class label, rather than simply receiving a class-conditional vector as auxiliary inputs. Suppose there are  $|\mathcal{S}|$  candidates of the generator architecture, and the dataset contains  $M$  object classes, then the total number of possible combinations is  $|\mathcal{S}|^M$ . We need an efficient algorithm to explore the large space.

We make use of neural architecture search (NAS), a recently popular methodology that investigates finding the optimal architecture(s) among a large number of candidates [43]. But we notice some differences from this problem and the standard vision tasks (*e.g.*, image classification) for NAS evaluation. The major one lies in the need of distributing data and computation over a potentially large number of classes. Directly transplanting a naive training strategy (*e.g.*, individually optimizing

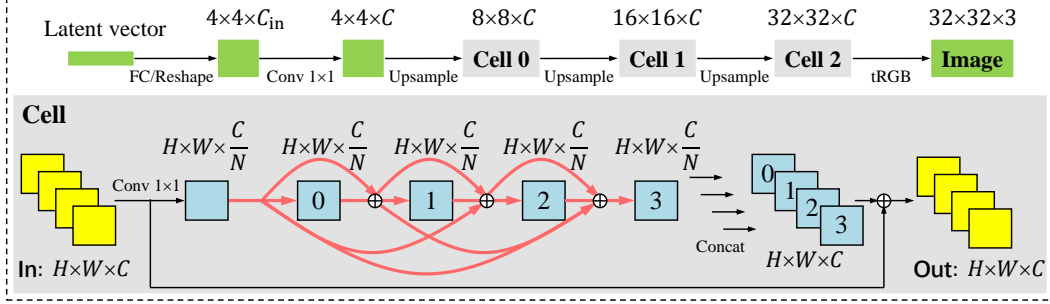


Figure 1: A tentative architecture in the search space.  $N$  stands for the number of nodes in a cell, set to 4 as an example. The operators shown in red arrows can be searched. The data shape is unchanged within each cell, so that the number of cells can be arbitrary. This figure is best viewed in color.

the architecture for each class) incurs heavy computational burden and lack of training data. In what follows, we elaborate how to design the search space and the search method, so that data and computation are maximally shared among classes and the search efficiency is largely improved.

### 3.2 Search Space: Sharing Data by Class-Modulated Convolution

The design of the search space follows the popular cell-based style. The input latent vector is passed through  $L$  up-sampling layers, each of which is followed by a cell that does not change the shape (spatial resolution and channel number) of the data. Each contains an input node, an output node, and  $N$  intermediate nodes and there exists an edge between each pair of nodes, propagating neural responses from the lower-indexed node to the higher-indexed node. Each node summarizes inputs from its precedents, *i.e.*,  $\mathbf{x}_j = \sum_{i < j} o_{i,j}(\mathbf{x}_i)$  where  $o_{i,j}(\cdot)$  is the operator on edge  $(i, j)$ , chosen from the set of candidate operators,  $\mathcal{O}$ . To guarantee that the shape of data is unchanged, at the beginning of each cell, the data is pre-processed using a  $1 \times 1$  convolutional layer that shrinks the number of channels by a factor of  $N$ . Hence, the output of intermediate nodes, after being concatenated, recover the original data shape. An architecture with tentative operators is shown in Figure 1.

Since the operator used in each edge can be searched, the number of different architectures is  $|\mathcal{O}|^{L \times \binom{N+1}{2}}$ . Note that we allow each class to have a distinct architecture, therefore, if there are  $M$  classes in the dataset, the total number of possible combinations is  $|\mathcal{O}|^{L \times \binom{N+1}{2} \times M}$ . This is quite a large number. Even with the simplest setting used in this paper (*i.e.*,  $|\mathcal{O}| = 2$ ,  $L = 3$ ,  $N = 2$ ), this number is  $2^{90} \approx 1.2 \times 10^{27}$  for a 10-class dataset (*e.g.*, CIFAR10) or  $2^{900} \approx 8.5 \times 10^{270}$  for a 100-class dataset (*e.g.*, CIFAR100), much larger than some popular cell-based search spaces (*e.g.*, the DARTS space [26, 5, 40] with  $1.1 \times 10^{18}$  architectures).

#### 3.2.1 Class-Modulated Convolution

The first challenge we encounter is that the training data need to be distributed among all classes. That being said, if the architectures of all classes are ‘truly’ independent (*e.g.*, all network weights are individually optimized), the amount of training data for each architecture, compared to the scenario that all classes share the same architecture, is reduced by a factor of  $M$ . This can result in severe over-fitting and unsatisfying performance of image generation.

To alleviate this risk, we share training data among different architectures by reusing model weights. In practice, most network weights are contributed by the convolutional layers, so we maintain one set of convolutional kernels and use a light-weighted module to introduce class-conditional information. Inspired by CBN [8] and the ‘demodulation’ operation [22], we propose the **class-modulated convolution** (*CMconv*) operator to incorporate class-conditional information. As shown in Figure 2, a *CMconv* layer consists of three parts, modulation, demodulation, and convolution. The *CMconv* shares convolutional weights with the corresponding regular convolution (*Rconv*).

Mathematically, let  $\mathbf{x}$  denote the input features maps with a class label of  $y$ , and  $\omega$  represent the weights of convolution. The goal of *modulation* is to introduce a scale factor to each of the input channels, *i.e.*,  $\omega' = \omega \odot \mathbf{s}_{\text{in}}$  where both  $\omega$  and  $\omega'$  are in a shape of  $c_{\text{in}} \times c_{\text{out}} \times U$ . Here,  $c_{\text{in}}$

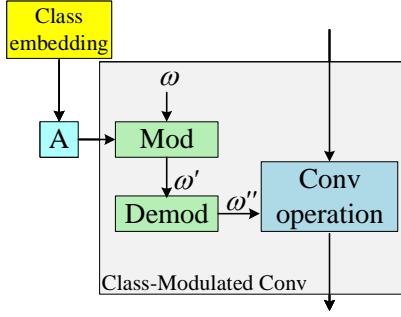


Figure 2: A class-modulated convolution, where the class-conditional vector (class embedding) is used to modulate the convolutional weights (shared with the regular convolution).

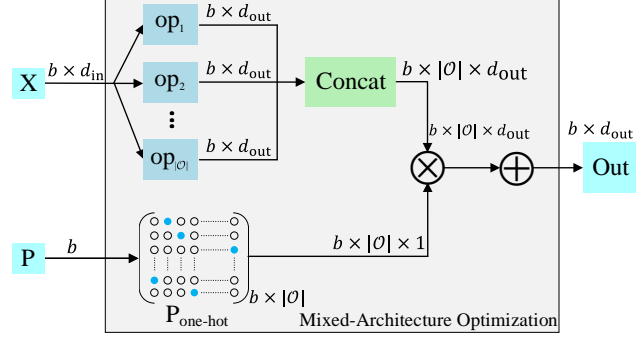


Figure 3: The mixed-architecture optimization with parallelization in a mini-batch.  $\otimes$  stands for tensor-broadcasting multiplication, and  $\oplus$  represents sum along the second dimension of the input

and  $c_{\text{out}}$  are the number of input and output channels, respectively, and  $U$  is the kernel size (e.g.,  $3 \times 3$ );  $\mathbf{s}_{\text{in}}$  is a  $c_{\text{in}}$ -dimensional vector and  $\omega \odot \mathbf{s}_{\text{in}}$  multiplies each set of weights ( $c_{\text{out}} \times U$  numbers) by the corresponding entry in  $\mathbf{s}_{\text{in}}$ . We follow the conventional formulation of cGAN to define  $\mathbf{s}_{\text{in}}$  as an affine-transformed class vector, i.e.,  $\mathbf{s}_{\text{in}} = \text{Aff}(\mathbf{e}_y)$ , where  $\text{Aff}(\cdot)$  is simply implemented as a trainable fully-connected layer and  $\mathbf{e}_y$  is a learnable embedding vector of the class label,  $y$ . The goal of *demodulation* is to normalize the weights and keep the variance of the input and output features same. We follow [22] to use  $\omega'' = \omega' \odot \mathbf{s}_{\text{out}}^{-1}$  where  $\mathbf{s}_{\text{out}}$  is a  $c_{\text{out}}$ -dimensional vector and  $\mathbf{s}_{\text{out}}^{-1}$  indicates element-wise reciprocal;  $\mathbf{s}_{\text{out}}$  is similar to the  $\ell_2$ -norm of  $\omega'$ , computed as  $\mathbf{s}_{\text{out}} = \sqrt{\sum_{c_{\text{in}}, u} (\omega'_{c_{\text{in}}, u})^2 + \epsilon}$ , where  $\epsilon$  is a small constant to avoid numerical instability.

In summary, *Rconv* and *CMconv* start with the same weight,  $\omega$ , and *CMconv* modulates  $\omega$  into  $\omega''$ . Then, regular convolution is performed, i.e.,  $\text{conv}(\mathbf{x}; \omega)$  or  $\text{conv}(\mathbf{x}; \omega'')$ . Since modulation and demodulation introduce relatively fewer parameters compared to convolution, so using weight-sharing *Rconv* and *CMconv* operators in each edge is a safe option that enables the limited amount of training data to be shared among a large number of generators.

### 3.3 Search Method: Sharing Computation by Mixed-Architecture Optimization

The search process is formulated by a one-step Markov Decision Process (MDP). We denote  $a$  as the action that samples architectures for all classes. Let  $\pi(a; \theta) \in (0, 1)$  be the sampling policy and  $\theta$  the learnable parameters, the performance of  $\pi(a; \theta)$  is measured by:

$$J(\theta) = \mathbb{E}_{a \sim \pi(a; \theta)} [R(a)], \quad (1)$$

where  $R(a)$  is the reward function. Throughout this paper, we use the Inception Score as the reward. According to REINFORCE [39], the gradient of  $J(\theta)$  with respect to  $\theta$  can be computed as:

$$\nabla_{\theta} J(\theta) = \mathbb{E}_{a \sim \pi(a; \theta)} [(R(a) - r) \cdot \nabla_{\theta} \log(\pi(a; \theta))] \approx \frac{1}{m} \sum_{k=1}^m (R(a_k) - r) \cdot \nabla_{\theta} \log(\pi(a_k; \theta)), \quad (2)$$

where  $m$  is the number of sampled architectures and  $r$  is a baseline reward, set to be the moving average and used to reduce the variance in the training process. We use gradient ascent to maximize  $J(\theta)$ . Inspired by [4, 41], we design a simple policy. We use  $\theta_{l,k}$  to denote a  $|\mathcal{O}|$ -dimensional parameter of class  $k$  and layer  $l$ , so that the probability of sampling each operator,  $\text{Prob}(o|\theta_{l,k})$ , is determined by the softmax output of  $\theta_{l,k}$ . Hence, given class-aware architectures,  $A_{\text{ca}}$ , the probability that it gets sampled is  $\text{Prob}(A_{\text{ca}}|\pi(a; \theta)) = \prod_{l,k} \text{Prob}(o|\theta_{l,k})$ .

### 3.3.1 Optimization: Search, Re-Training, and Calibration

There are two sets of parameters to be learned, *i.e.*,  $\theta$  for the sampling policy and  $\omega$  for the super-network. We use the hinge adversarial loss [25]:

$$\begin{aligned}\mathcal{L}_D &= \mathbb{E}_{q(y)} [\mathbb{E}_{q(\mathbf{x}|y)} [\max\{0, 1 - D(\mathbf{x}, y)\}] + \mathbb{E}_{q(y)} [\mathbb{E}_{p(\mathbf{z})} [\max\{0, 1 + D(G(\mathbf{z}, y), y)\}]], \\ \mathcal{L}_G &= -\mathbb{E}_{q(y)} [\mathbb{E}_{p(\mathbf{z})} [D(G(\mathbf{z}, y), y)]],\end{aligned}\tag{3}$$

where  $\mathbf{x}$  with class label  $y$  is sampled from the real dataset,  $D(\cdot)$  and  $G(\cdot)$  denote the discriminator and generator, respectively, and  $p(\mathbf{z})$  is the standard Gaussian distribution. We use the discriminator in AutoGAN [13] and add class projection (*cproj* [29]) to it. **We emphasize that *cproj* is critical to our algorithm (please refer to Section 4.4.2).**

During the **search** phase, we adopt the weight-sharing NAS approach [32] to optimize the generator, *i.e.*, the super-network parameterized by  $\omega$ . We perform fair sampling strategy [7] to offer equal opportunity for training each generator architecture. After every  $T_{\text{critic}} = 5$  iterations, we update the generator weights; after every  $T_{\text{policy}} = 50$  iterations, we update the policy parameters,  $\theta$ . The pseudo code of the optimization process is provided in Appendix A.

After the search is done, we obtain the generator architecture for each class by choosing the operator with the largest score on each edge, *i.e.*,  $o_{l,k} = \arg \max_o \text{Prob}(o|\theta_{l,k})$ . Then, we **re-train** the generator from scratch following the same procedure. The last step is named **calibration**, in which we fine-tune the each architecture on the corresponding class for a small number of iterations (thus the overhead is small). As we will show in experiments, the calibration step largely boosts the performance, because the re-training stage has pursued for the optimality over all classes, which does not necessarily align with the optimality on each individual class.

### 3.3.2 Sharing Computation: Mixed-Architecture Optimization

We notice a technical issue that greatly downgrades the efficiency of both search and re-training. Given a mini-batch,  $\mathcal{B}$ , from the training set, as  $\mathcal{B}$  may contain features from multiple classes, they need to be propagated through different architectures. To avoid heavy computational burden<sup>2</sup>, we propose **mixed-architecture optimization** to allow different architectures to be optimized within one forward-then-backward pass in a batch.

The flowchart of mixed-architecture optimization is shown in Figure 3. Let  $\mathbf{X}$  denote a batch of input features of size  $b \times d_{\text{in}}$ , where  $b$  is the size of the batch,  $\mathcal{B}$ , and  $d_{\text{in}}$  is the feature dimensionality. To improve the efficiency of parallelization,  $\mathbf{X}$  as a whole is propagated through every operator, and each training sample chooses the output corresponding to the selected operator. In practice, this is implemented by concatenating all the outputs of  $o(\mathbf{X})$ ,  $o \in \mathcal{O}$ , and multiply it by  $\mathbf{P}$ , a  $b \times |\mathcal{O}|$  indicator matrix. Each row of which is a one-hot,  $|\mathcal{O}|$ -dimensional vector indicating the operator selected by the corresponding sample.

Essentially, mixed-architecture optimization performs redundant computation to achieve more efficient parallelization. Each input feature is fed into all  $|\mathcal{O}|$  operators, though only one of the outputs will be used. Nevertheless,  $b \times |\mathcal{O}|$  does not increase with the number of classes and thus our method generalizes well to complex datasets, *e.g.*, CIFAR100.

## 4 Experiments

### 4.1 Dataset, Evaluation, and Implementation Details

We use CIFAR10 and CIFAR100 [24] as the testbeds. Both datasets have 50,000 training and 10,000 testing images, uniformly distributed over 10 or 100 classes. We use the Inception Score (IS) [36] and the Fréchet Inception Distance (FID) [16] to measure the performance of GAN on 50K randomly generated images. The FID statistic files are pre-calculated using all training images. We also compute the FID score within each class of CIFAR10. Specifically, for each class, we first use 5K

<sup>2</sup>If we deal with each class in a batch individually, the corresponding architectures need to be loaded to the GPU one by one and the batch size becomes small, which results in a reduction in computational efficiency. Moreover, inefficiency deteriorates with the number of classes increases.

Table 1: FID scores of class-agnostic and class-aware GANs on CIFAR10.

Method	Intra FIDs ↓										FID ↓
	<i>airp.</i>	<i>auto.</i>	<i>bird</i>	<i>cat</i>	<i>deer</i>	<i>dog</i>	<i>frog</i>	<i>horse</i>	<i>ship</i>	<i>truck</i>	
NAS-cGAN	29.10	13.62	26.64	22.21	14.97	26.02	17.32	15.18	14.99	16.58	7.05
NAS-cGAN (calibrated)	26.83	13.05	25.99	21.24	14.56	23.39	17.32	15.17	14.46	14.99	6.63
NAS-caGAN	29.53	12.32	24.83	21.30	16.11	26.64	16.56	16.79	16.43	16.39	6.83
NAS-caGAN (calibrated)	25.36	<b>11.91</b>	<b>22.66</b>	<b>19.63</b>	<b>13.74</b>	23.29	<b>15.81</b>	15.60	13.82	<b>14.78</b>	<b>5.85</b>
NAS-caGAN-light	35.21	12.64	29.04	24.96	21.20	26.26	18.62	16.40	14.87	18.67	7.79
NAS-caGAN-light (calibrated)	<b>23.90</b>	12.69	24.13	23.36	18.39	<b>22.12</b>	16.93	<b>14.71</b>	<b>13.17</b>	15.01	6.31

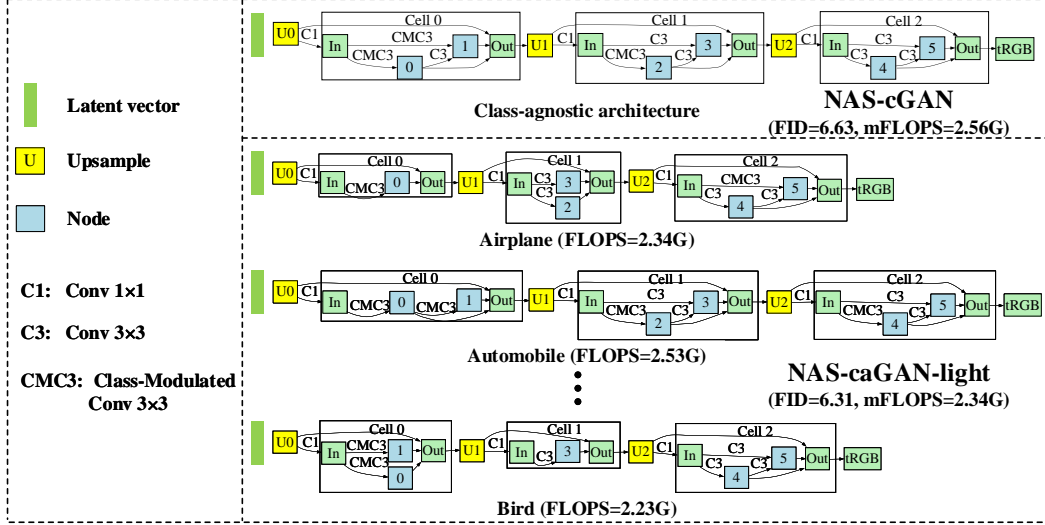


Figure 4: Part of the generator architectures found by NAS-caGAN-light on the CIFAR10 dataset. Compared to the class-agnostic architecture (shown at the top), the class-aware architectures enjoy a lower FID score as well as cheaper computation. This figure is best viewed in color.

real training images to pre-calculate the statistic file, and then randomly generate another 5K images for computing the intra FID score.

For all experiments, we use the Adam optimizer [23] with  $\eta = 0.0001$ ,  $\beta_1 = 0$ , and  $\beta_2 = 0.9$  for optimizing GAN, and  $\eta = 0.00035$ ,  $\beta_1 = 0.9$ , and  $\beta_2 = 0.999$  for policy learning. For the discriminator, we adopt the same architecture used in AutoGAN [13], but equip it with the *cproj* [29]. The discriminator is updated five times per update of the generator. All experiments are performed on a GeForce GTX-1080Ti GPU, with the batch size set to be 32. We search for 200K iterations and re-train for 500K iterations that are sufficient to achieve stable results.

## 4.2 Class-Aware Image Generation on CIFAR10

Table 1 summarizes the image generation results on CIFAR10. We use NAS-cGAN to denote the method that each class uses the same searched generator architecture, and NAS-caGAN to denote the method with class-aware generators incorporated. The former option is achieved by a modified version of the proposed search algorithm that the sampling policy is shared among all classes. It can be seen that NAS-caGAN produces lower FID scores, indicating its better performance compared to NAS-cGAN. After calibration, NAS-caGAN achieves even better results, reporting an FID of 5.85 that is the best known to date. We also compare the calibrated versions of NAS-cGAN and NAS-caGAN and find that the latter is better, indicating that both class-aware architectures and calibration contribute to the generating better images.

We notice that the current space chooses each operator between *RConv* and *CMConv*, both of which are parameterized and expensive. To find computationally efficient architectures, we add the *zero* operator into the search space, and without any further modification, derive a light-weighted version of class-aware generators, denoted as NAS-caGAN-light. With or without calibration, NAS-caGAN-

light achieves comparable FID values, while enjoying a reduced average computational overhead (2.34G FLOPs vs. 2.56G FLOPs) of NAS-caGAN. This is another merit of using class-aware architectures. Figure 4 shows part of the generator architectures found by NAS-caGAN-light. More architecture details are shown in Appendix B.

### 4.3 Results on CIFAR100

Next, we challenge our method by evaluating it on CIFAR100 which has much more classes. Thanks to the proposed mixed-architecture optimization, we can perform architecture search on CIFAR100 without additional engineering efforts compared to that on CIFAR10. Differently, we do not perform calibration or evaluate the intra-class FID scores, since there are only 500 training images for each class, which is insufficient to approximate the true image distribution.

Still, we use NAS-cGAN and NAS-caGAN to denote the class-agnostic and class-aware versions of cGAN, respectively. Table 2 summarizes the results. Again, by allowing different classes to have individual generator architectures, NAS-caGAN achieves better performance in terms of both the FID and IS scores. Note that NAS-caGAN significantly outperforms cproj [29] which uses a hand-crafted generator network. The searched architectures are shown in Appendix C.

Table 2: FID and IS values of class-agnostic and class-aware GANs on CIFAR100.

Method	FID ↓	IS ↑
cproj [29]	23.20	9.04
NAS-cGAN	13.94	8.83 ± 0.09
NAS-caGAN	<b>12.28</b>	<b>9.71 ± 0.09</b>

## 4.4 Diagnostic Studies

### 4.4.1 Unconditional Image Generation on CIFAR10

We first study the effectiveness of the search space and the search algorithm. We design two class-agnostic versions in the architecture that we have used in the above experiments. The first one is to directly set all operators to be *RConv*, and the second is to search a common architecture for all classes, with each the operator on each edge chosen among *RConv*, *skip-connect*, and *zero*. Note that we remove the *CMConv* operator to guarantee that class information is NOT used at all. The discriminator is also class-agnostic with the same architecture used in AutoGAN (without *cproj*).

Table 3: Comparison between existing automatically designed GAN methods and our algorithm in the setting that all classes share the same generator architecture. No class label is used at all.

Method	Params (M)	FID ↓	IS ↑
AGAN [38]	20.1	30.50	8.29 ± 0.09
AutoGAN [13]	4.4	12.42	8.55 ± 0.10
AdversarialNAS [11]	8.8	10.87	<b>8.74 ± 0.07</b>
baseline (full)	6.0	12.26	8.61 ± 0.07
NAS-GAN (searched)	5.4	<b>10.80</b>	8.32 ± 0.09

Results are summarized in Table 3. We deliver two messages. First, our search space that contains 9 selectable operators seems small, but has sufficient ability to find powerful models and compete against recently published methods. Second, the searched NAS-GAN preserves most parameterized operator (*RConv*), showing that GAN needs a sufficient amount parameters to achieve good performance. This supports the design of our search space, *i.e.*, the competition is held between two parameterized operators. The searched architecture is shown in Appendix D.

### 4.4.2 Importance of the Class-Projection Discriminator

Based on the NAS-caGAN model, we investigate the difference between using a normal discriminator (*i.e.*, no class information) and using a class-projection (*cproj*) discriminator [29]. On CIFAR10, these models report FID scores of 15.90 and 6.83, respectively, *i.e.*, the *cproj* discriminator is significantly better. We owe the performance gain to the ability that *cproj* induces more *CMConv* operators. As shown in Figure 5a, the normal discriminator leads to a sparse use of *CMConv* operators, while, as in Figure 5b, *CMConv* occupies almost half of the operators when *cproj* is used. That being said, the class-aware generators should be searched under the condition that the discriminator is also class-aware. This aligns with the results obtained in [29], showing that one usually uses the *cproj* discriminator together with the generator containing conditional batch normalization (CBN) operations.

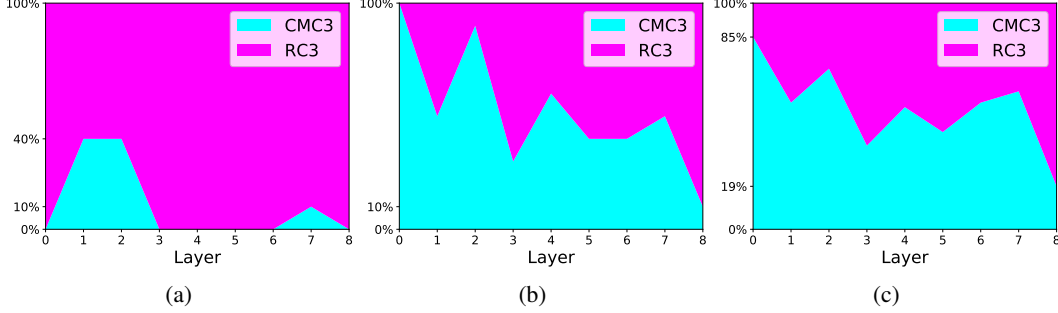


Figure 5: The proportion of *RConv* and *CMConv* in each layer of the searched class-aware architectures, where (a) is obtained using a normal discriminator on CIFAR10, (b) is obtained using a *cproj* discriminator on CIFAR10, and (c) is obtained using a *cproj* discriminator on CIFAR100. See Section 4.4 for details.

#### 4.4.3 Where Shall We Place Class-Aware Operators?

Last but not least, we study how our algorithm assigns the class-aware operator (*i.e.*, *CMConv*) to different positions of the searched generator architectures. Continuing the previous study, we plot the portion of *CMConv* on CIFAR100 in Figure 5c, which shows a very similar trend as the experiments on CIFAR10. In particular, the portion for the first operator (close to the input noise vector) to use *CMConv* is 100% on CIFAR10 and 85% on CIFAR100, while the portion for the last operator (close to the output generated image) is only 10% and 19% on CIFAR10 and CIFAR100, respectively. This is to suggest that class information seems very important for capturing the distribution of high-level semantics (close to input), while all classes seem to share similar low-level patterns (close to output).

To verify that the finding can indeed enhance GAN models, we experiment on BigGAN [3], a manually designed GAN model. The generator of BigGAN uses three blocks on CIFAR10, each of which contains two class-conditional operations (*i.e.*, CBN) by default. We perform experiments by using CBN only in the first or the last block but replacing all other CBN with regular BN. As shown in Figure 6, the model that uses CBN only in the first block (close to input) works better than the baseline (*i.e.*, using CBN in all blocks), but the model that uses CBN only in the last block (close to output) produces inferior performance. That being said, our finding in the automatic search procedure sheds new light on the optimization of manually designed GAN models.

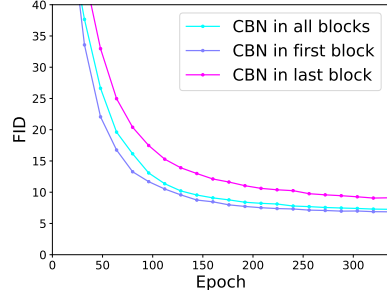


Figure 6: Evaluating the BigGAN architecture on CIFAR10 with CBN inserted into different blocks. Please refer to the main texts for details.

## 5 Conclusions

In this paper, we discuss the possibility of designing class-aware generators for conditional GAN models. Though the motivation seems straightforward, it requires non-trivial technical efforts to improve the performance as well as efficiency of the algorithm, in particular when the number of classes becomes large. We claim two key contributions. **First**, the search space containing regular and class-modulated convolutions eases the re-training process because all convolutional weights can be trained on the full dataset. **Second**, we design a mix-architecture optimization mechanism so that the search and re-training processes can be performed efficiently. In a relatively small search space, our algorithm achieves FID scores of 5.85 and 12.28 on CIFAR10 and CIFAR100, respectively, both of which are the best numbers known to date. Provided more computational resources, our algorithm has the potential of generating images of higher quality.

Our research leaves some open problems to the community. First, we have used the constraint that all operators are either regular or class-modulated convolution. This is to improve the efficiency of utilizing training data, but this also limits the diversity of the searched generator architectures. Second, it is interesting to jointly optimize the architectures of generator and discriminator, since we have found strong evidence of their cooperation. We leave these topics to future work.

## Broader Impact

This paper presents a NAS method for designing class-aware generator architectures for cGAN. We summarize the potential impact of our work in the following aspects.

- **To the research community.** We verify the possibility of designing and training cGAN models with different generators for all classes. This is a new direction for the research community and we believe that follow-up researchers can extend our approach to more cGAN-based vision tasks.
- **To the downstream engineers.** Our method is efficient and consistently improves the performance of cGAN models. With the code released to public, our algorithm has the potential of being applied to a wide range of real-world image generation applications. While this may help to develop AI-based applications, there exist risks that some engineers, with relatively less knowledge in deep learning and GAN, can deliberately use the algorithm and result in worse generation results.
- **To the society.** There is a long-lasting debate on the impact that AI can bring to the human society. In particular, GAN-based algorithms have raised serious concerns of being used for improper scenarios, *e.g.*, generating fake images or videos. Therefore, in general, it can bring both beneficial and harmful impacts and it really depends on the motivation of the users.

We also encourage the community to investigate the following problems.

1. Are there better solutions for the class-aware generators and the discriminator to cooperate with each other?
2. Is there any need of exploring the usage of mixed-architecture optimization in the discriminator, so that it allows the samples in a batch to use different network architectures?
3. Is it possible to apply the class-modulated convolution (*CMconv*) to other image translation tasks, *e.g.*, style transfer, attribute transfer, *etc.*?

## References

- [1] M. Arjovsky, S. Chintala, and L. Bottou. Wasserstein Generative Adversarial Networks. In *ICML*, 2017.
- [2] S. Arora, R. Ge, Y. Liang, T. Ma, and Y. Zhang. Generalization and Equilibrium in Generative Adversarial Nets (GANs). *arXiv:1703.00573 [cs, stat]*, 2017.
- [3] A. Brock, J. Donahue, and K. Simonyan. Large scale gan training for high fidelity natural image synthesis. *arXiv:1809.11096*, 2018.
- [4] H. Cai, L. Zhu, and S. Han. ProxylessNAS: Direct Neural Architecture Search on Target Task and Hardware. In *ICLR*, 2019.
- [5] X. Chen, L. Xie, J. Wu, and Q. Tian. Progressive Differentiable Architecture Search: Bridging the Depth Gap between Search and Evaluation. In *ICCV*, 2019.
- [6] X. Chen, L. Xie, J. Wu, L. Wei, Y. Xu, and Q. Tian. Fitting the Search Space of Weight-sharing NAS with Graph Convolutional Networks. *arXiv:2004.08423 [cs, stat]*, 2020.
- [7] X. Chu, B. Zhang, R. Xu, and J. Li. FairNAS: Rethinking Evaluation Fairness of Weight Sharing Neural Architecture Search. *arXiv:1907.01845 [cs, stat]*, 2019.
- [8] H. de Vries, F. Strub, J. Mary, H. Larochelle, O. Pietquin, and A. Courville. Modulating early visual processing by language. In *NeurIPS*, 2017.
- [9] E. Denton, S. Chintala, A. Szlam, and R. Fergus. Deep Generative Image Models using a Laplacian Pyramid of Adversarial Networks. *arXiv:1506.05751 [cs]*, 2015.
- [10] I. Durugkar, I. Gemp, and S. Mahadevan. Generative Multi-Adversarial Networks. In *ICLR*, 2017.
- [11] C. Gao, Y. Chen, S. Liu, Z. Tan, and S. Yan. AdversarialNAS: Adversarial Neural Architecture Search for GANs. *arXiv:1912.02037 [cs, eess]*, 2019.

- [12] A. Ghosh, V. Kulharia, V. Namboodiri, P. H. S. Torr, and P. K. Dokania. Multi-Agent Diverse Generative Adversarial Networks. In *CVPR*, 2018.
- [13] X. Gong, S. Chang, Y. Jiang, and Z. Wang. AutoGAN: Neural Architecture Search for Generative Adversarial Networks. In *ICCV*, 2019.
- [14] I. Goodfellow, J. Pouget-Abadie, M. Mirza, B. Xu, D. Warde-Farley, S. Ozair, A. Courville, and Y. Bengio. Generative Adversarial Nets. In *NeurIPS*, 2014.
- [15] I. Gulrajani, F. Ahmed, M. Arjovsky, V. Dumoulin, and A. C. Courville. Improved training of wasserstein gans. In *NeurIPS*, 2017.
- [16] M. Heusel, H. Ramsauer, T. Unterthiner, B. Nessler, and S. Hochreiter. GANs Trained by a Two Time-Scale Update Rule Converge to a Local Nash Equilibrium. In *NeurIPS*, 2017.
- [17] Q. Hoang, T. D. Nguyen, T. Le, and D. Phung. MGAN: Training Generative Adversarial Nets with Multiple Generators. In *ICLR*, 2018.
- [18] A. Jolicœur-Martineau. The relativistic discriminator: A key element missing from standard GAN. In *ICLR*, 2019.
- [19] A. Karnewar and O. Wang. MSG-GAN: Multi-Scale Gradient GAN for Stable Image Synthesis. *arXiv:1903.06048 [cs, stat]*, 2019.
- [20] T. Karras, T. Aila, S. Laine, and J. Lehtinen. Progressive Growing of GANs for Improved Quality, Stability, and Variation. *arXiv:1710.10196 [cs, stat]*, 2017.
- [21] T. Karras, S. Laine, and T. Aila. A Style-Based Generator Architecture for Generative Adversarial Networks. In *CVPR*, 2019.
- [22] T. Karras, S. Laine, M. Aittala, J. Hellsten, J. Lehtinen, and T. Aila. Analyzing and Improving the Image Quality of StyleGAN. *arXiv:1912.04958 [cs, eess, stat]*, 2019.
- [23] D. P. Kingma and J. Ba. Adam: A Method for Stochastic Optimization. In *ICLR*, 2014.
- [24] A. Krizhevsky, G. Hinton, et al. Learning multiple layers of features from tiny images. Technical report, Citeseer, 2009.
- [25] J. H. Lim and J. C. Ye. Geometric GAN. *arXiv:1705.02894 [cond-mat, stat]*, 2017.
- [26] H. Liu, K. Simonyan, and Y. Yang. DARTS: Differentiable Architecture Search. In *ICLR*, 2019.
- [27] X. Mao, Q. Li, H. Xie, R. Y. K. Lau, Z. Wang, and S. P. Smolley. Least Squares Generative Adversarial Networks. *arXiv:1611.04076 [cs]*, 2016.
- [28] M. Mirza and S. Osindero. Conditional Generative Adversarial Nets. *arXiv:1411.1784 [cs, stat]*, 2014.
- [29] T. Miyato and M. Koyama. cGANs with Projection Discriminator. In *ICLR*, 2018.
- [30] T. Nguyen, T. Le, H. Vu, and D. Phung. Dual discriminator generative adversarial nets. In *NeurIPS*, 2017.
- [31] A. Odena, C. Olah, and J. Shlens. Conditional Image Synthesis With Auxiliary Classifier GANs. *arXiv:1610.09585 [cs, stat]*, 2017.
- [32] H. Pham, M. Y. Guan, B. Zoph, Q. V. Le, and J. Dean. Efficient Neural Architecture Search via Parameter Sharing. In *ICML*, 2018.
- [33] G.-J. Qi. Loss-Sensitive Generative Adversarial Networks on Lipschitz Densities. *arXiv:1701.06264 [cs]*, 2017.
- [34] A. Radford, L. Metz, and S. Chintala. Unsupervised Representation Learning with Deep Convolutional Generative Adversarial Networks. *arXiv:1511.06434 [cs]*, 2015.
- [35] S. Reed, Z. Akata, X. Yan, L. Logeswaran, B. Schiele, and H. Lee. Generative Adversarial Text to Image Synthesis. In *ICML*, 2016.
- [36] T. Salimans, I. Goodfellow, W. Zaremba, V. Cheung, A. Radford, X. Chen, and X. Chen. Improved Techniques for Training GANs. In *NeurIPS*, 2016.
- [37] I. Tolstikhin, S. Gelly, O. Bousquet, C.-J. Simon-Gabriel, and B. Schölkopf. AdaGAN: Boosting Generative Models. *arXiv:1701.02386 [cs, stat]*, 2017.
- [38] H. Wang and J. Huan. AGAN: Towards Automated Design of Generative Adversarial Networks. *arXiv:1906.11080 [cs, stat]*, 2019.

- [39] R. J. Williams. Simple statistical gradient-following algorithms for connectionist reinforcement learning. *Machine Learning*, 8(3), 1992.
- [40] Y. Xu, L. Xie, X. Zhang, X. Chen, G.-J. Qi, Q. Tian, and H. Xiong. Pc-darts: Partial channel connections for memory-efficient architecture search. In *ICLR*, 2020.
- [41] C. Ying, A. Klein, E. Real, E. Christiansen, K. Murphy, and F. Hutter. NAS-Bench-101: Towards Reproducible Neural Architecture Search. *arXiv:1902.09635 [cs, stat]*, 2019.
- [42] H. Zhang, I. Goodfellow, D. Metaxas, and A. Odena. Self-Attention Generative Adversarial Networks. *arXiv:1805.08318 [cs, stat]*, 2018.
- [43] B. Zoph and Q. V. Le. Neural Architecture Search with Reinforcement Learning. *arXiv:1611.01578*, 2016.

## A Search Algorithm

Algorithm 1 shows the pseudo-code of the search procedure. As shown on line 2, we employ fair sampling strategy [7] to offer equal opportunity for training each child model of the super-network. However, unlike FairNAS [7] performing architecture search after the training of the super-network, our method embed the search process (policy learning) into the training loop of the super-network (shown on line 12). This is equivalent to performing a moving average for the policy parameters over the course of training. Based on NAS-caGAN model, we investigate the difference between these two search strategies. On CIFAR10, these models report FID scores of 6.83 and 7.61, respectively, *i.e.*, our proposed search strategy is better. We attribute the performance gain to the moving average for the policy parameters that could reduce the ranking noise of the weight-sharing NAS [6].

Thanks to the proposed mixed-architecture optimization, the search procedure can be very simple regardless of the number of classes. As shown on line 8, mixed-architecture optimization allows class image generation with distinct generating architectures in a single forward pass. That is to say, although each class may have varied generator architecture, these architectures can forward in parallel so that the training process is as simple as that of the original GAN [14].

---

**Algorithm 1** Searching with mixed-architecture optimization (pseudo-code in a PyTorch style).

---

```

#  $N_{\text{op}}$       :the number of operators in a searched edge
#  $L$          :the number of searched edges in an architecture
#  $N_{\text{critic}}$     :the number of times for updating the discriminator per update of the generator
#  $N_{\text{policy}}$     :update policy every  $N_{\text{policy}}$  iterations
#  $N_c$         :the number of classes

1: for iter, ( $\mathbf{x}, y$ ) in enumerate(data_loader): # images  $\mathbf{x} : (b, c, h, w)$ , class label  $y : (b, )$ 
    # prepare a batch of network architectures
2:   fair_arcs = fair_arc_sampling() # fair_arcs :  $(N_{\text{op}}, L)$ , derived by the fair sampling
3:   arcs = fair_arcs.repeat(b, 1) # arcs :  $(b \times N_{\text{op}}, L)$ 

    # broadcast inputs to ensure each sample goes through fair_arcs
4:    $\mathbf{x} = \mathbf{x}.\text{repeat\_interleave}(\text{repeats} = N_{\text{op}}, \text{dim} = 0)$  #  $\mathbf{x} : (b \times N_{\text{op}}, c, h, w)$ 
5:    $y = y.\text{repeat\_interleave}(\text{repeats} = N_{\text{op}}, \text{dim} = 0)$  #  $y : (b \times N_{\text{op}}, )$ 

    # update super-network parameters  $\omega$  (we simplify the notation by omitting the noise  $z$ )
6:   update_D( $\mathbf{x}, y, \text{arcs}$ )
7:   if iter %  $N_{\text{critic}} == 0$ :
8:     update_G( $y, \text{arcs}$ )

    # update policy parameters  $\theta$ 
9:   if iter %  $N_{\text{policy}} == 0$ :
    # sample generator architectures by the policy for all classes
10:    class_arcs = arc_sampling_by_policy() # class_arcs :  $(N_c, L)$ 
11:    reward = eval_InceptionScore(class_arcs)
12:    update_policy(reward)

Return: policy  $\pi(a; \theta)$ 

```

---

## B Searched Generator Architectures on CIFAR-10

### B.1 Generator architectures for NAS-cGAN and NAS-caGAN

We use  $RConv_{3 \times 3}$  and  $CMConv_{3 \times 3}$  as candidate operators. These operators and their corresponding index numbers are shown in Table 4. On CIFAR10, there are three cells for a generator architecture, each of which contains two nodes, so there are three edges to be searched in a cell and nine edges in total. The searched generator architectures of NAS-cGAN and NAS-caGAN are shown in Table 5. It can be seen that the class conditional operator ( $CMConv$ ) tends to appear at the shallow layers (close to the input noise vector), and the class unrelated operator ( $RConv$ ) prefers to appear at

the output layers (close to the generated images). This phenomenon is definitely suggestive for future studies on the design of generator architectures.

Table 4: Candidate operators for NAS-cGAN and NAS-caGAN

Index	Operator
0	$RConv\_3 \times 3$ (regular convolution)
1	$CMConv\_3 \times 3$ (class-modulated convolution)

Table 5: Searched architectures for NAS-cGAN and NAS-caGAN

Method	Class	Layer									
		0	1	2	3	4	5	6	7	8	
NAS-cGAN	<i>All</i>	1	1	0	1	0	0	0	0	0	
NAS-caGAN	0	1	1	0	0	0	0	0	0	0	
	1	1	1	1	0	0	1	0	1	0	
	2	1	0	1	0	1	1	0	0	1	
	3	1	1	1	0	0	1	1	1	0	
	4	1	0	1	0	1	0	0	1	0	
	5	1	0	1	1	1	1	1	1	0	
	6	1	0	1	0	1	0	1	0	0	
	7	1	0	1	1	1	0	0	1	0	
	8	1	1	1	1	1	0	1	0	0	
	9	1	1	1	0	0	0	0	0	0	

## B.2 Generator architectures for NAS-caGAN-light

We add a non-parameter operator, *zero*, to the search space, and derive a light-weighted version of class-aware generators, named NAS-caGAN-light. Table 6 and 7 present the operators with index numbers and searched architectures, respectively. As shown in Table 7, the distribution of  $RConv$  and  $CMConv$  still conforms to the rules mentioned in Sec. B.1.

Class-aware generator architectures enjoy another merit that different classes could have varied computational overhead. Figure 7 shows the computational overhead of each class on CIFAR10. It can be seen that NAS-caGAN is superior to NAS-cGAN in terms of FID score. Both models have almost the same computational overhead for all classes because all the candidate operators are parameterized ( $RConv$  and  $CMConv$ ). After incorporating the non-parameter operator, NAS-caGAN-light achieves comparable FID score with NAS-cGAN, but with less computational overhead. The visualization of the class-aware generators of NAS-caGAN-light is presented in Figure 8.

Table 6: Candidate operators for NAS-caGAN-light

Index	Operator
0	<i>zero</i>
1	$RConv\_3 \times 3$ (regular convolution)
2	$CMConv\_3 \times 3$ (class-modulated convolution)

Table 7: Searched architectures for NAS-caGAN-light

Method	Class	Layer									
		0	1	2	3	4	5	6	7	8	
NAS-caGAN-light	0	2	0	0	1	1	0	1	2	1	
	1	2	0	2	2	1	1	2	1	1	
	2	2	2	0	0	1	0	1	1	1	
	3	2	0	1	0	1	1	1	1	1	
	4	0	1	0	2	1	1	1	1	0	
	5	2	0	1	0	1	1	2	1	2	
	6	2	2	0	0	1	0	1	2	1	
	7	2	0	0	2	1	1	2	1	1	
	8	2	2	0	2	0	1	2	2	1	
	9	2	1	1	2	1	1	1	1	1	

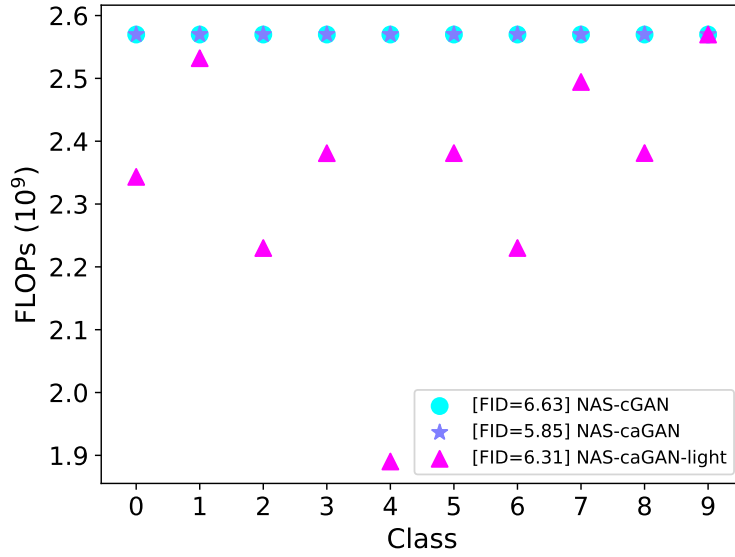


Figure 7: The computational overhead of each class on CIFAR10. Under comparable FLOPs, NAS-caGAN is superior to NAS-cGAN in terms of FID score. Under comparable FID score, NAS-caGAN-light has fewer FLOPs than NAS-cGAN for each class.

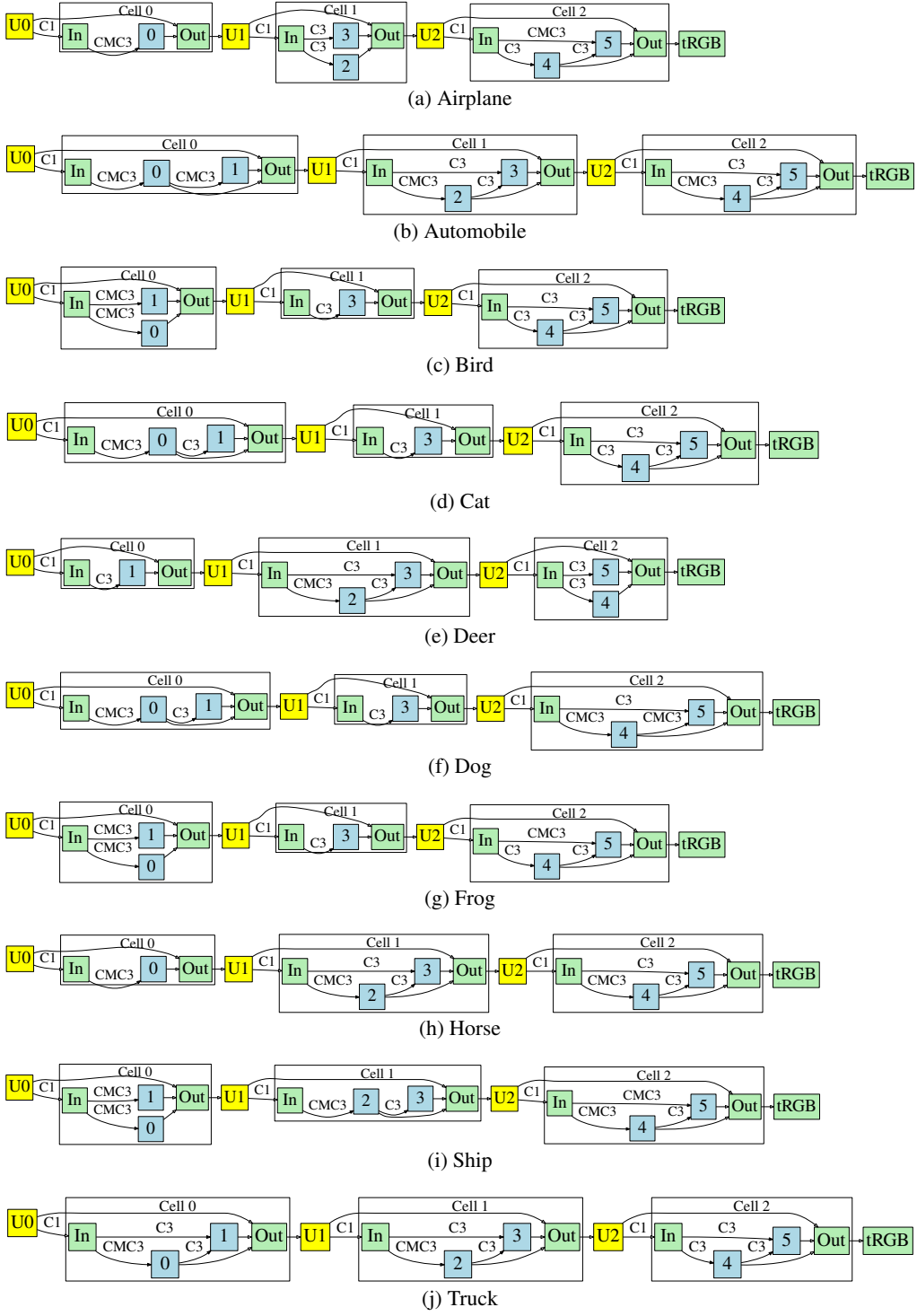


Figure 8: Visualization of class-aware generators of NAS-caGAN-light

## C Searched Generator Architectures on CIFAR-100

We perform experiments on CIFAR100, using the same search space and hyper-parameters as in CIFAR10, except increasing the number of classes to 100. That is to say, there will be more policy parameters for the search of NAS-caGAN. We emphasize that owing to the mixed-architecture optimization, the search and retraining programs can be applied to this setting with more classes without any modification. The candidate operators and searched architectures are shown in Table 8 and Table 9, respectively. One can see from Table 9 that the distribution of *RConv* and *CMConv* still conforms to the rules discussed in Sec. B.1.

Table 8: Candidate operators for NAS-cGAN and NAS-caGAN

Index	Operator
0	<i>RConv</i> <sub>3 × 3</sub> (regular convolution)
1	<i>CMConv</i> <sub>3 × 3</sub> (class-modulated convolution)

Table 9: Searched architectures for NAS-cGAN and NAS-caGAN

Method	Class	Layer									
		0	1	2	3	4	5	6	7	8	
NAS-cGAN	All	1	1	0	1	0	1	1	1	0	
NAS-caGAN	0	1	1	1	1	0	1	1	0	0	
	1	1	0	0	0	0	1	0	1	1	
	2	1	1	1	0	1	0	1	1	0	
	3	1	1	1	1	0	1	1	1	0	
	4	1	0	1	1	0	0	1	1	0	
	5	1	1	1	0	0	0	0	0	0	
	6	1	1	0	0	0	0	1	0	0	
	7	1	1	0	1	1	1	1	1	1	
	8	1	0	1	0	1	1	0	0	0	
	9	1	1	0	0	0	0	1	1	1	
	10	1	1	1	1	1	1	0	0	0	
	11	1	0	1	1	1	1	0	1	0	
	12	1	0	0	0	1	0	1	1	0	
	13	1	1	1	0	1	1	0	1	0	
	14	1	0	1	0	1	0	1	1	0	
	15	1	0	0	1	1	0	1	1	0	
	16	1	1	0	1	0	1	0	1	0	
	17	1	0	1	0	1	0	1	1	0	
	18	0	0	0	0	0	1	1	0	0	
	19	1	1	1	1	1	0	0	1	0	
	20	1	1	1	0	0	1	1	1	0	
	21	1	0	1	1	1	1	1	1	0	
	22	1	0	1	0	0	1	0	1	1	
	23	1	0	1	1	1	1	1	1	1	
	24	1	0	1	1	1	0	1	0	0	
	25	1	0	1	0	0	0	0	1	0	
	26	1	1	1	1	0	0	1	1	0	
	27	1	1	1	0	1	0	1	1	0	
	28	1	1	1	0	0	0	1	1	0	
	29	1	1	0	0	1	0	0	0	0	
	30	1	1	1	1	1	0	1	1	0	
	31	1	0	1	1	0	0	1	1	0	
	32	0	1	1	0	0	0	0	0	0	
	33	1	0	0	0	1	0	0	1	1	
34	1	1	0	0	0	0	1	0	0		

35	1	1	1	1	1	0	0	1	0
36	0	1	1	1	0	1	0	0	1
37	1	0	1	0	1	0	0	0	0
38	1	1	1	1	0	0	1	1	0
39	1	0	1	0	1	1	1	1	0
40	1	1	1	0	1	0	1	0	0
41	1	0	1	0	1	0	0	0	0
42	1	0	1	0	1	0	1	0	0
43	1	1	1	1	1	1	1	1	0
44	1	0	0	1	1	0	1	1	0
45	0	1	0	0	1	1	0	1	0
46	1	1	1	1	1	0	0	0	0
47	0	0	1	0	0	0	0	1	0
48	1	1	1	0	1	1	0	1	0
49	1	1	0	1	1	1	1	1	1
50	1	1	1	1	1	0	1	1	0
51	1	0	0	0	1	1	1	1	0
52	1	1	0	0	0	0	1	1	0
53	1	1	1	1	1	1	1	0	1
54	1	0	1	0	0	0	0	1	0
55	1	0	0	0	1	1	0	0	0
56	1	1	1	0	0	0	0	0	0
57	1	1	1	0	0	1	0	0	0
58	1	1	0	0	0	0	0	1	0
59	1	1	1	0	0	0	1	1	0
60	1	1	1	0	1	0	1	1	0
61	1	0	1	0	1	0	0	0	0
62	0	0	1	0	0	1	0	0	1
63	0	0	0	1	0	0	1	1	0
64	1	0	1	1	1	1	1	0	1
65	0	0	1	1	0	0	1	0	0
66	1	0	1	0	0	1	1	1	0
67	1	0	1	1	0	1	1	1	1
68	0	1	1	0	0	0	1	0	0
69	1	1	1	0	1	0	1	1	0
70	1	0	1	1	0	0	0	0	1
71	1	1	1	1	1	1	1	1	0
72	1	0	0	1	0	1	1	1	1
73	1	1	0	1	0	1	1	1	1
74	0	1	1	1	0	0	1	1	0
75	1	0	1	1	0	1	1	1	0
76	1	0	1	0	1	1	0	1	0
77	1	0	0	1	1	0	1	0	0
78	1	0	1	0	1	0	0	1	0
79	1	1	1	0	1	1	0	0	0
80	1	1	1	0	0	0	1	0	0
81	1	1	0	0	1	0	0	0	0
82	0	1	1	0	0	1	1	1	0
83	1	0	1	0	0	1	0	0	0
84	1	0	0	0	0	0	0	0	0
85	1	1	0	0	1	0	0	1	0
86	1	0	0	0	1	0	0	1	0
87	1	1	1	0	0	1	0	0	1
88	1	0	1	0	0	0	1	1	0
89	1	1	1	0	1	0	0	1	0
90	1	1	0	0	1	0	0	1	0
91	0	1	1	0	1	1	1	0	1
92	0	1	1	0	1	1	1	1	1

93	1	1	1	0	0	1	0	0	1
94	1	0	1	0	0	0	0	1	0
95	1	1	0	1	1	1	1	1	0
96	0	1	0	0	1	0	0	0	0
97	1	1	1	0	1	0	1	0	0
98	1	0	1	1	1	1	0	0	0
99	0	1	1	0	0	1	1	0	0

## D Generator Architectures for Unconditional Image Generation

We evaluate the effectiveness of the search space and algorithm on the unconditional image generation task on CIFAR10. As shown in Table 10, we chose three candidate operators: *zero*, *skip-connect*, and *RConv*. We adopt the discriminator used in AutoGAN [13]. The entire processes of search and re-training do NOT use any class information at all.

Table 11 presents the searched architecture. The searched NAS-GAN achieves a better FID score than the baseline (10.80 vs. 12.26). Analyzing the architecture details, we can find that NAS-GAN preserves most parameterized operator (*RConv*), this phenomenon indicating that GAN model needs a sufficient number of parameters to achieve good performance. This supports the design of the search space of the class-aware generators, where the competition is held only between two parameterized operators.

Table 10: Candidate operators for NAS-GAN

Index	Operator
0	<i>zero</i>
1	<i>skip-connect</i>
2	<i>RConv</i> <sub>3 × 3</sub> (regular convolution)

Table 11: Architectures for baseline and NAS-GAN

Method	Class	Layer									
		0	1	2	3	4	5	6	7	8	
baseline (full)	<i>All</i>	2	2	2	2	2	2	2	2	2	
NAS-GAN (searched)	<i>All</i>	2	2	1	2	2	2	2	2	2	

## E Results of Class Conditional Image Generation

We show some generated images of NAS-caGAN models trained on CIFAR10 and CIFAR100, in Figure 9 and Figure 10, respectively. In the figures, each row corresponds to samples of one class. All the samples are randomly sampled rather than cherry-picked.

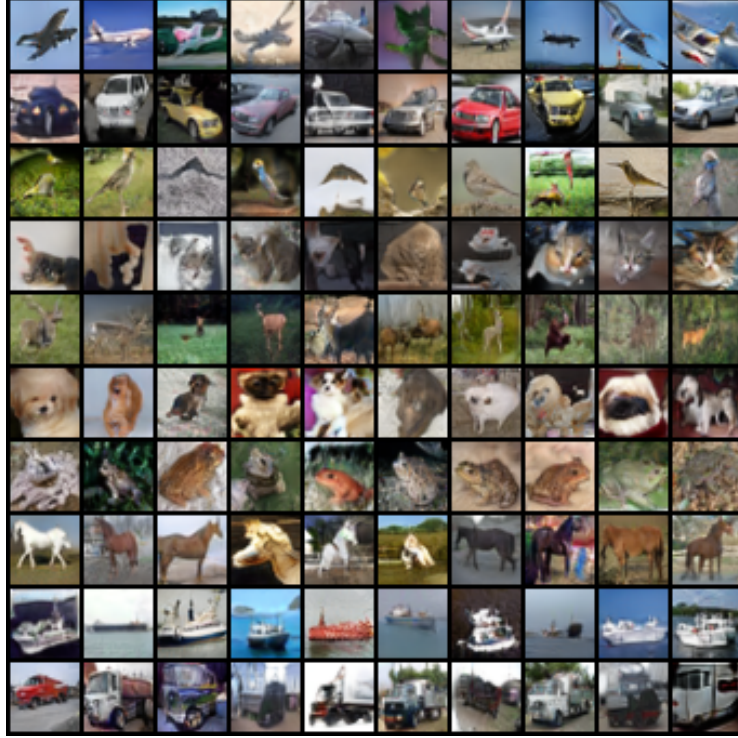


Figure 9: Generated images of NAS-caGAN model trained on CIFAR10. Each row corresponds to samples of the same class.



Figure 10: Generated images of NAS-caGAN model trained on CIFAR100. Each row corresponds to samples of the same class. Due to space limitations, we only show samples of 20 classes without cherry-picking.